Inhomogeneous phases in rotating gluon plasma

A. A. Roenko[1],

in collaboration with

V. V. Braguta, M. N. Chernodub,

[1] Joint Institute for Nuclear Research, Bogoliubov Laboratory of Theoretical Physics

roenko@theor.jinr.ru

The XIXth Workshop on High Energy Spin Physics
Dubna, 6 September 2023

The work was supported by RSF grant No. 23-10-00072.

JOINT INSTITUTE FOR NUCLEAR RESEARCH

- In non-central heavy ion collisions creation of QGP with angular momentum is expected.

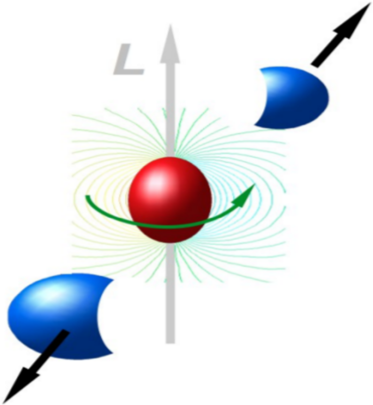

- In non-central heavy ion collisions creation of QGP with angular momentum is expected.
- The rotation occurs with relativistic velocities.

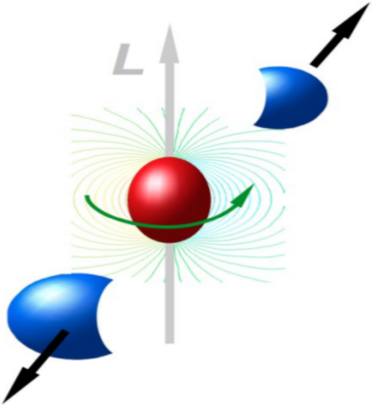

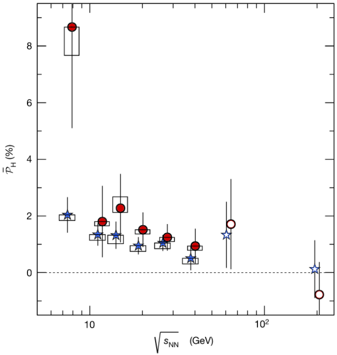

[L. Adamczyk et al. (STAR), Nature **548**, 62–65 (2017), arXiv:1701.06657 [nucl-ex]]

$\langle\omega\rangle \sim 6$ MeV $\;(\sqrt{s_{NN}}$-averaged)

All* theoretical models assume that the system rotates like rigid body, $\Omega \neq 0$.

Our lattice results for gluodynamics show that the confinement critical temperature increases with rotation

- V. V. Braguta, A. Y. Kotov, D. D. Kuznedelev, and A. A. Roenko, JETP Lett. **112**, 6–12 (2020)
- V. V. Braguta, A. Y. Kotov, D. D. Kuznedelev, and A. A. Roenko, Phys. Rev. D **103**, 094515 (2021), arXiv:2102.05084 [hep-lat]
- V. Braguta, A. Y. Kotov, D. Kuznedelev, and A. Roenko, PoS **LATTICE2021**, 125 (2022), arXiv:2110.12302 [hep-lat]

Lattice results for QCD: the chiral and deconfinement critical temperatures both increase with rotation (decrease with imaginary rotation); fermions and gluons have opposite influence on T_c.

- V. V. Braguta, A. Kotov, A. Roenko, and D. Sychev, PoS **LATTICE2022**, 190 (2023), arXiv:2212.03224 [hep-lat]

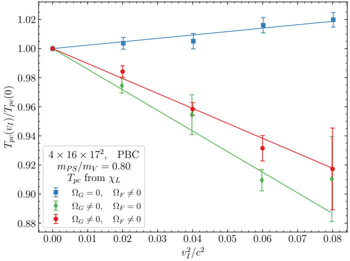

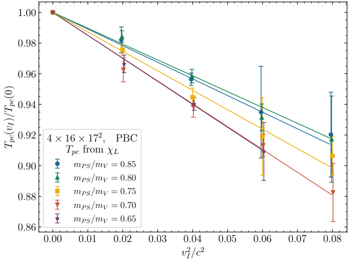

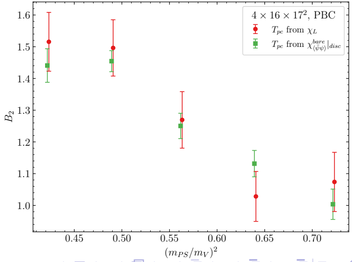

Critical temperature in rotating QCD

Recent lattice results with staggered fermions confirm our results for behavior of T_c in rotating QCD.

- J.-C. Yang and X.-G. Huang, (2023), arXiv:2307.05755 [hep-lat]

The NJL model with running effective coupling $G(\omega)$ gives a similar prediction: the critical temperature of the chiral transition increases due to the rotation.

- Y. Jiang, Eur. Phys. J. C **82**, 949 (2022), arXiv:2108.09622 [hep-ph]

Revolving bag model: the deconfinement critical temperature increases with angular velocity.

- K. Mameda and K. Takizawa, (2023), arXiv:2308.07310 [hep-ph]

Critical temperature in rotating QCD

Recent lattice results with staggered fermions confirm our results for behavior of T_c in rotating QCD.

- J.-C. Yang and X.-G. Huang, (2023), arXiv:2307.05755 [hep-lat]

The NJL model with running effective coupling $G(\omega)$ gives a similar prediction: the critical temperature of the chiral transition increases due to the rotation.

- Y. Jiang, Eur. Phys. J. C **82**, 949 (2022), arXiv:2108.09622 [hep-ph]

Revolving bag model: the deconfinement critical temperature increases with angular velocity.

- K. Mameda and K. Takizawa, (2023), arXiv:2308.07310 [hep-ph]

Inhomogeneous phases (the results for local T_c is consistent with the Tolman-Ehrenfest effect):

2+1 cQED:

- M. N. Chernodub, Phys. Rev. D **103**, 054027 (2021), arXiv:2012.04924 [hep-ph]

Holography:

- N. R. F. Braga and O. C. Junqueira, (2023), arXiv:2306.08653 [hep-th]

Lattice formulation of rotating QCD

We study quenched QCD in the co-rotating reference frame (it rotates with angular velocity Ω around z-axis) $\to$ external gravitational field [A. Yamamoto and Y. Hirono, Phys. Rev. Lett. **111**, 081601 (2013), arXiv:1303.6292 [hep-lat]]

$$g^E_{\mu\nu} = \begin{pmatrix} 1 & 0 & 0 & x_2\Omega_I \\ 0 & 1 & 0 & -x_1\Omega_I \\ 0 & 0 & 1 & 0 \\ x_2\Omega_I & -x_1\Omega_I & 0 & 1 + x_\perp^2\Omega_I^2 \end{pmatrix}, \tag{1}$$

where $x_\perp^2 = x_1^2 + x_2^2$, and the angular velocity is put in the purely imaginary form $\Omega_I = -i\Omega$ to avoid the sign problem. The partition function is

$$Z = \int DA \, \exp\left(- S_G[A, \Omega]\right). \tag{2}$$

We use the lattices with size $N_t \times N_z \times N_s^2$.

The gluon action has the following form:

$$S = \frac{1}{4g_0^2}\int d^4x\,\sqrt{g_E}\,g_E^{\mu\nu}g_E^{\alpha\beta}F^a_{\mu\alpha}F^a_{\nu\beta} \equiv S_0 + S_1\Omega_I + S_2\frac{\Omega_I^2}{2}\,, \tag{3}$$

where

$$S_0 = \frac{1}{4g_0^2}\int d^4x F^a_{\mu\nu}F^a_{\mu\nu}\,, \tag{4}$$

$$S_1 = \frac{1}{g_0^2}\int d^4x\,[x_2F^a_{12}F^a_{24} + x_2F^a_{13}F^a_{34} - x_1F^a_{21}F^a_{14} - x_1F^a_{23}F^a_{34}]\,, \tag{5}$$

$$S_2 = \frac{1}{g_0^2}\int d^4x\left[x_\perp^2(F^a_{12})^2 + x_2^2(F^a_{13})^2 + x_1^2(F^a_{23})^2 + 2x_1x_2F^a_{13}F^a_{32}\right], \tag{6}$$

Lattice formulation of rotating QCD

The gluon action has the following form:

$$S = \frac{1}{4g_0^2}\int d^4x\,\sqrt{g_E}\,g_E^{\mu\nu}g_E^{\alpha\beta}F^a_{\mu\alpha}F^a_{\nu\beta} \equiv S_0 + S_1\Omega_I + S_2\frac{\Omega_I^2}{2}\,, \tag{3}$$

where

$$S_0 = \frac{1}{4g_0^2}\int d^4x F^a_{\mu\nu}F^a_{\mu\nu}\,, \tag{4}$$

$$S_1 = \frac{1}{g_0^2}\int d^4x\,[x_2F^a_{12}F^a_{24} + x_2F^a_{13}F^a_{34} - x_1F^a_{21}F^a_{14} - x_1F^a_{23}F^a_{34}]\,, \tag{5}$$

$$S_2 = \frac{1}{g_0^2}\int d^4x\big[x_\perp^2(F^a_{12})^2 + x_2^2(F^a_{13})^2 + x_1^2(F^a_{23})^2 + 2x_1x_2F^a_{13}F^a_{32}\big], \tag{6}$$

Sign problem

- The Euclidean action is complex-valued function with real rotation ($S_1 \neq 0$)!
- The Monte–Carlo simulations are conducted with imaginary angular velocity $\Omega_I = -i\Omega$.
- The results are analytically continued to the region of the real angular velocity ($\Omega_I^2 = -\Omega^2$, $v_I^2 = -v_R^2$).

Polyakov loop

The Polyakov loop is an order parameter in gluodynamics.

$$L(x,y) = \frac{1}{N_z}\sum_z \mathrm{Tr}\left[\prod_{\tau=0}^{N_t-1} U_4(\vec{r},\tau)\right], \qquad L = \frac{1}{N_s^2}\sum_{x,y} L(x,y)\,. \tag{7}$$

In confinement $\langle L\rangle = 0$; in deconfinement $\langle L\rangle \neq 0$ ($\mathbb{Z}_3$ center symmetry is broken).

Polyakov loop

The Polyakov loop is an order parameter in gluodynamics.

$$L(x,y) = \frac{1}{N_z} \sum_z \mathrm{Tr}\left[\prod_{\tau=0}^{N_t-1} U_4(\vec{r},\tau)\right], \qquad L = \frac{1}{N_s^2} \sum_{x,y} L(x,y)\,. \tag{7}$$

In confinement $\langle L\rangle = 0$; in deconfinement $\langle L\rangle \neq 0$ ($\mathbb{Z}_3$ center symmetry is broken).

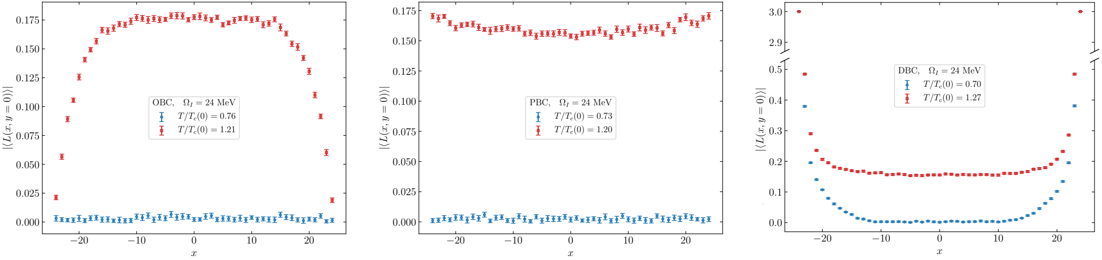

Figure: [from V. V. Braguta, A. Y. Kotov, D. D. Kuznedelev, and A. A. Roenko, Phys. Rev. D **103**, 094515 (2021), arXiv:2102.05084 [hep-lat]] The lattice $8 \times 24 \times 49^2$.

The spatial distributions of the local Polyakov loop have signs of inhomogeneity, the boundary is screened. To investigate the inhomogeneity in the vicinity of the phase transition large lattice size is needed.

With an increase in the temperature, the deconfinement phase arises from periphery.

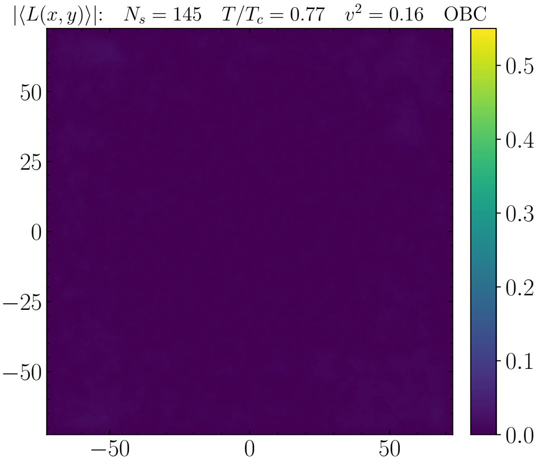

Lattice
$4 \times 24 \times 145^2$;

Velocity at the boundary
$v_I = \Omega_I R = \Omega_I L_s/2 \equiv 0.4$

Deconfinement phase transition in large rotating system

With an increase in the temperature, the deconfinement phase arises from periphery.

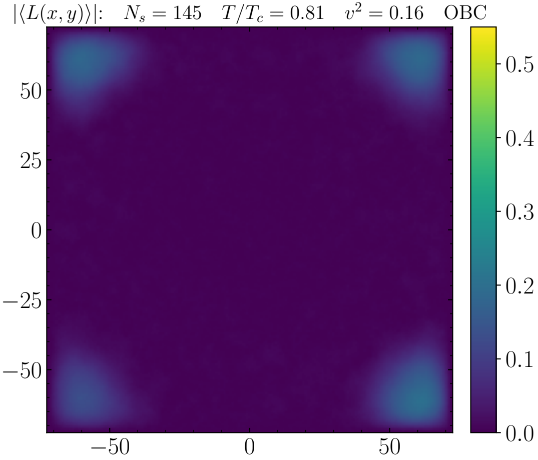

Lattice
$4 \times 24 \times 145^2$;

Velocity at the boundary
$v_I = \Omega_I R = \Omega_I L_s/2 \equiv 0.4$

With an increase in the temperature, the deconfinement phase arises from periphery.

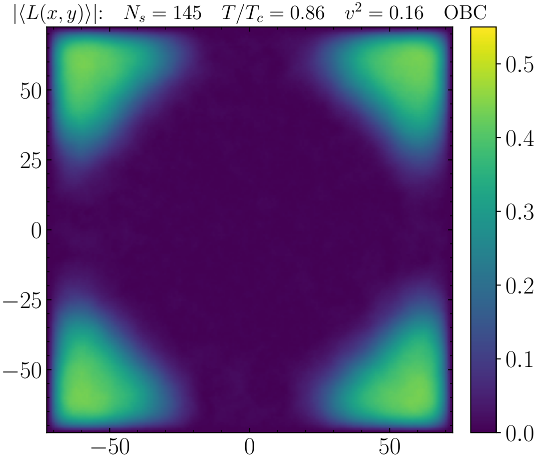

Lattice
$4 \times 24 \times 145^2$;

Velocity at the boundary
$v_I = \Omega_I R = \Omega_I L_s/2 \equiv 0.4$

Deconfinement phase transition in large rotating system

With an increase in the temperature, the deconfinement phase arises from periphery.

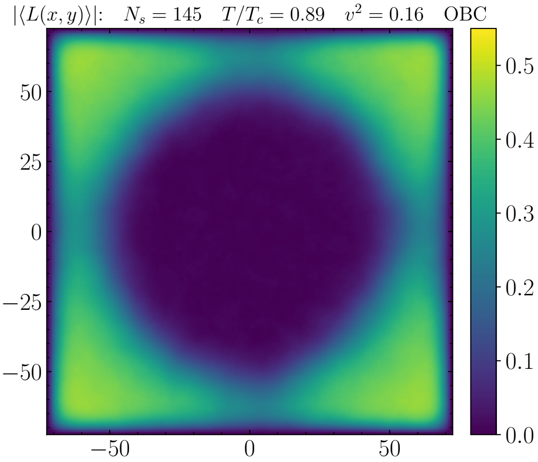

Lattice
$4 \times 24 \times 145^2$;

Velocity at the boundary
$v_I = \Omega_I R = \Omega_I L_s/2 \equiv 0.4$

Deconfinement phase transition in large rotating system

With an increase in the temperature, the deconfinement phase arises from periphery.

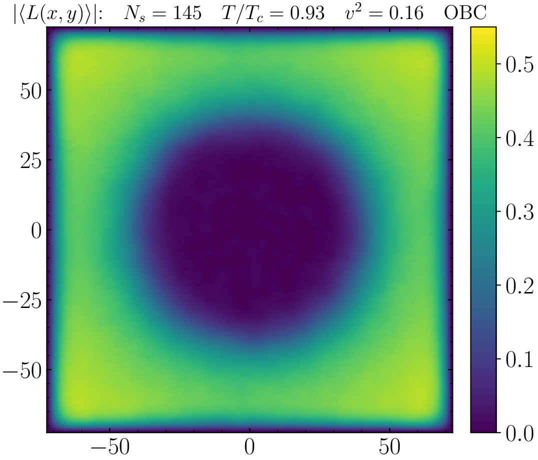

Lattice
$4 \times 24 \times 145^2$;

Velocity at the boundary
$v_I = \Omega_I R = \Omega_I L_s/2 \equiv 0.4$

Deconfinement phase transition in large rotating system

With an increase in the temperature, the deconfinement phase arises from periphery.

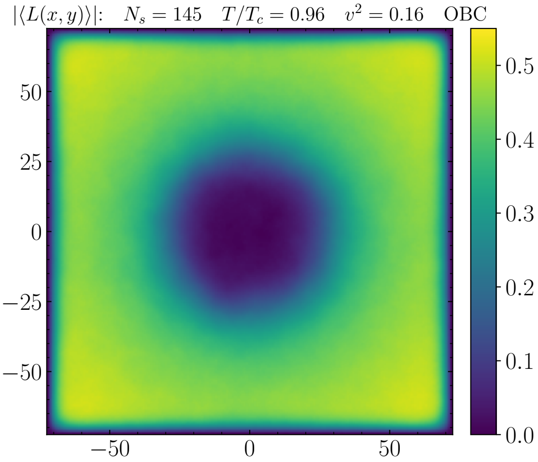

Lattice
$4 \times 24 \times 145^2$;

Velocity at the boundary
$v_I = \Omega_I R = \Omega_I L_s/2 \equiv 0.4$

With an increase in the temperature, the deconfinement phase arises from periphery.

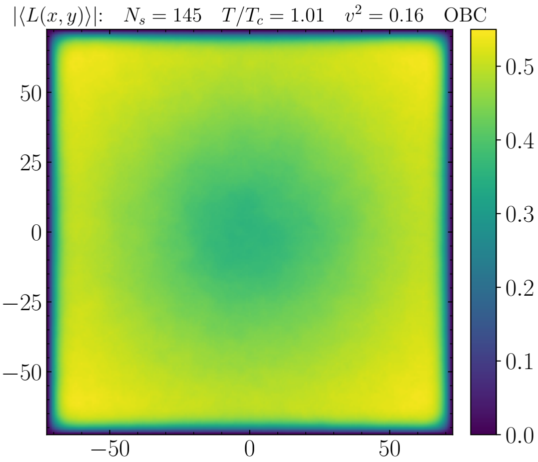

Lattice
$4 \times 24 \times 145^2$;

Velocity at the boundary
$v_I = \Omega_I R = \Omega_I L_s/2 \equiv 0.4$

Deconfinement phase transition in large rotating system

With an increase in the temperature, the deconfinement phase arises from periphery.

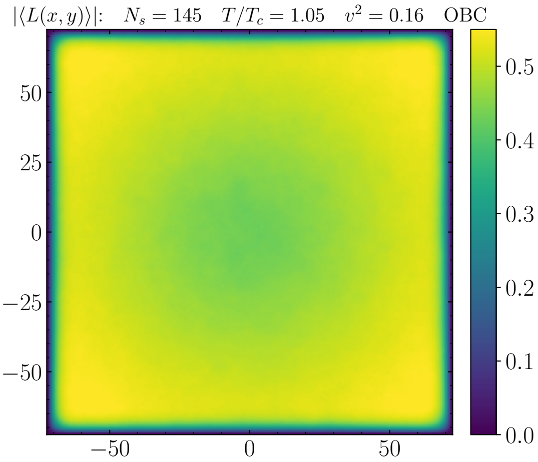

Lattice
$4 \times 24 \times 145^2$;

Velocity at the boundary
$v_I = \Omega_I R = \Omega_I L_s/2 \equiv 0.4$

Mixed-phase: influence of the boundary

The Polyakov loop distributions in the bulk is not affected by boundaries:

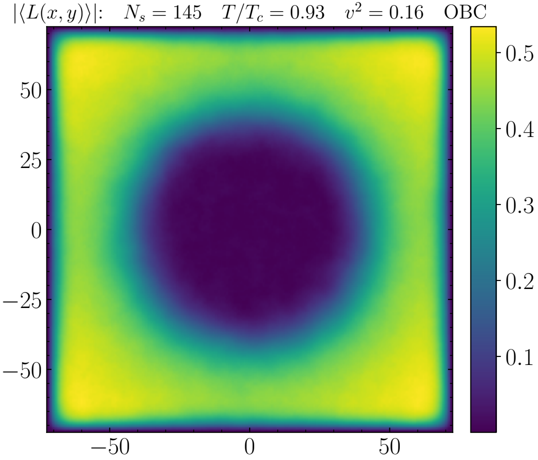

Lattice
$4 \times 24 \times 145^2$;

Velocity at the boundary
$v_I = \Omega_I R = \Omega_I L_s/2 \equiv 0.4$

Angular velocity
$\Omega_I = 6.08$ MeV

"Radius" of the system
$R = L_s/2 = a(N_s - 1)/2 = 13$ fm

Lattice spacing
$a = 0.18$ fm

The Polyakov loop distributions in the bulk is not affected by boundaries:

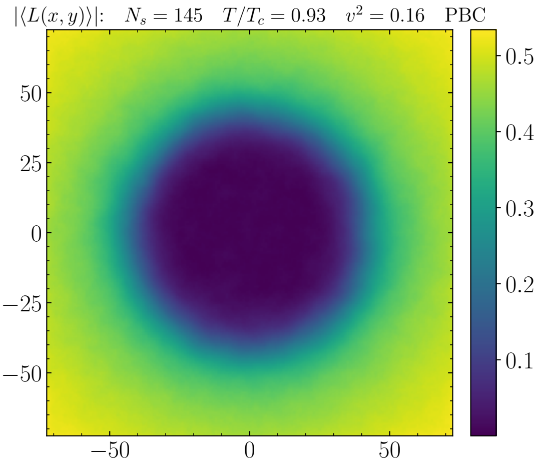

Lattice
$4 \times 24 \times 145^2$;

Velocity at the boundary
$v_I = \Omega_I R = \Omega_I L_s/2 \equiv 0.4$

Angular velocity
$\Omega_I = 6.08$ MeV

"Radius" of the system
$R = L_s/2 = a(N_s - 1)/2 = 13$ fm

Lattice spacing
$a = 0.18$ fm

Mixed-phase: influence of the boundary

The Polyakov loop distributions in the bulk is not affected by boundaries:

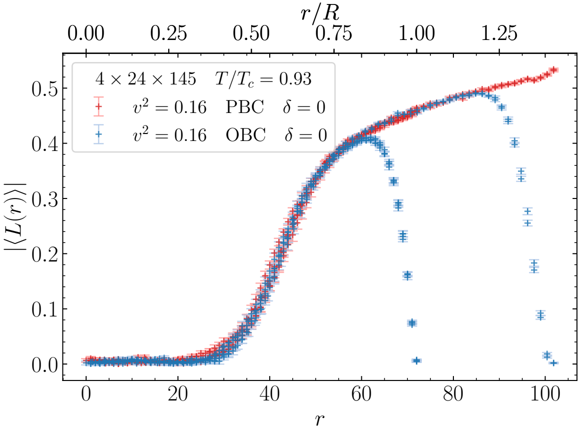

Lattice
$4 \times 24 \times 145^2$;

Velocity at the boundary
$v_I = \Omega_I R = \Omega_I L_s/2 \equiv 0.4$

Angular velocity
$\Omega_I = 6.08$ MeV

"Radius" of the system
$R = L_s/2 = a(N_s - 1)/2 = 13$ fm

Lattice spacing
$a = 0.18$ fm

Mixed-phase: influence of the boundary

The Polyakov loop distributions in the bulk is not affected by boundaries:

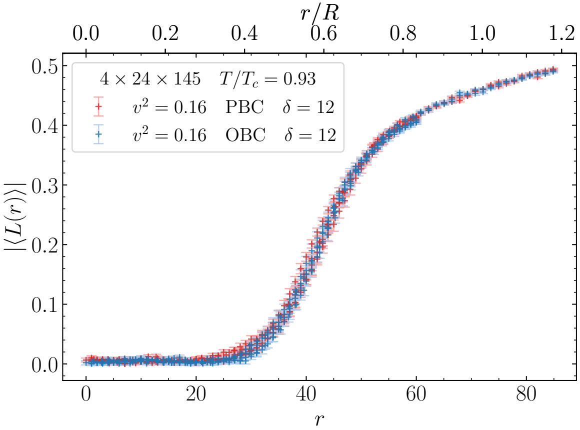

Lattice
$4 \times 24 \times 145^2$;

Velocity at the boundary
$v_I = \Omega_I R = \Omega_I L_s/2 \equiv 0.4$

Angular velocity
$\Omega_I = 6.08$ MeV

"Radius" of the system
$R = L_s/2 = a(N_s - 1)/2 = 13$ fm

Lattice spacing
$a = 0.18$ fm

The $\delta b = 12 = 3N_t$ sites are skipped from boundary (~ 2 fm).

The width of the transitions region is $\sim 25 \simeq 6N_t$ lattice steps (~ 4 fm). $\Rightarrow$ $\boxed{N_s/N_t \gtrsim 18}$

The Polyakov loop distributions mainly depend on the local velocity for a given temperature:

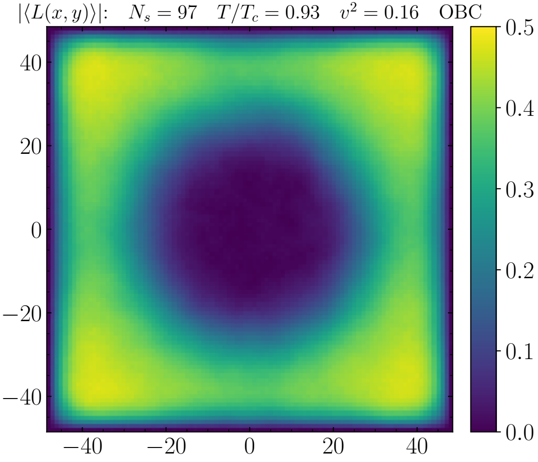

Lattice
$4 \times 24 \times 97^2$ $N_s/N_t = 24$

Velocity at the boundary
$v_I = \Omega_I R \equiv 0.4$

Angular velocity
$\Omega_I = 9.12$ MeV

"Radius" of the system
$R = L_s/2 = a(N_s - 1)/2 = 8.65$ fm

Lattice spacing
$a = 0.18$ fm

Mixed-phase: universal behaviour

The Polyakov loop distributions mainly depend on the local velocity for a given temperature:

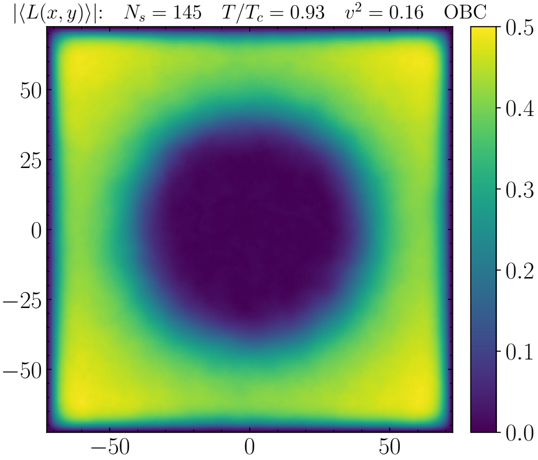

Lattice
$4 \times 24 \times 145^2$ $\quad N_s/N_t = 36$

Velocity at the boundary
$v_I = \Omega_I R \equiv 0.4$

Angular velocity
$\Omega_I = 6.08$ MeV

"Radius" of the system
$R = L_s/2 = a(N_s - 1)/2 = 13$ fm

Lattice spacing
$a = 0.18$ fm

The Polyakov loop distributions mainly depend on the local velocity for a given temperature:

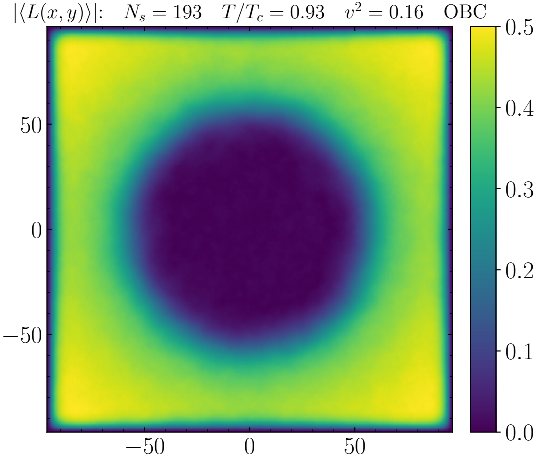

Lattice
$4 \times 24 \times 193^2 \qquad N_s/N_t = 48$

Velocity at the boundary
$v_I = \Omega_I R \equiv 0.4$

Angular velocity
$\Omega_I = 4.56$ MeV

"Radius" of the system
$R = L_s/2 = a(N_s - 1)/2 = 17.3$ fm

Lattice spacing
$a = 0.18$ fm

Mixed-phase: universal behaviour

The Polyakov loop distributions mainly depend on the local velocity for a given temperature:

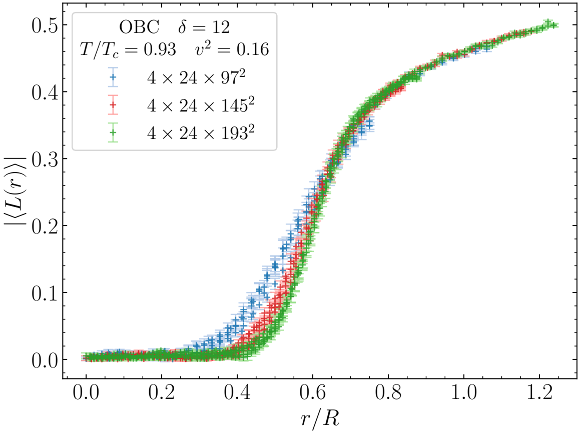

Velocity at the boundary
$v_I = \Omega_I R \equiv 0.4$

Lattice spacing
$a = 0.18$ fm

The transition becomes "sharper" (in relative units r/R) with increasing the transversal size R.
The position of the transition between different phases just slightly depends on the system size.

Local Polyacov loop susceptibility

We split our rotating system into subregions (circular layers) of constant width δr and measure the Polyakov loop and its susceptibility for these subregions. ($\delta r <$ width of transition)

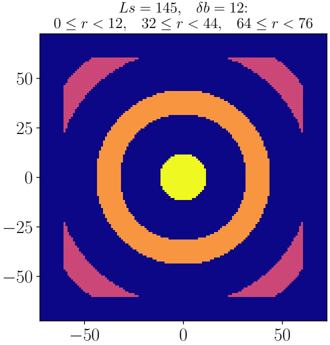

Local Polyacov loop susceptibility

We split our rotating system into subregions (circular layers) of constant width δr and measure the Polyakov loop and its susceptibility for these subregions. ($\delta r <$ width of transition)

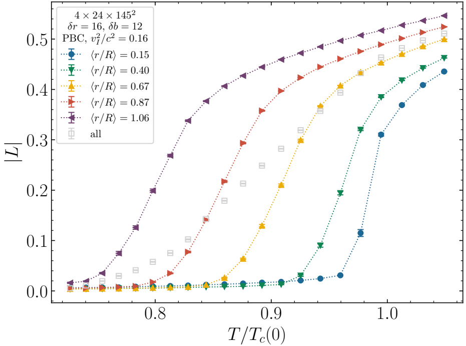

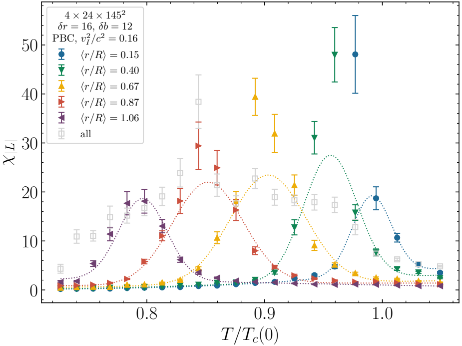

From this data, we find the local critical temperature using the Gaussian fit of the susceptibility.

Local critical temperature

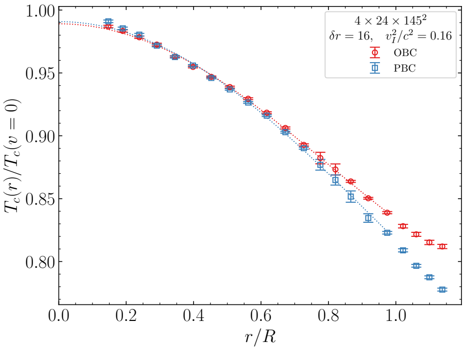

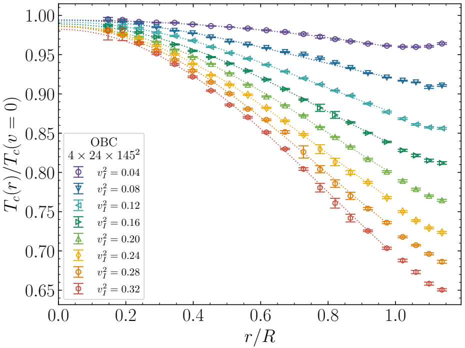

The results for local critical temperature are well described by two functions (we use points with $x = r/R < 1$ to reduce the boundary effects):

$$\frac{T_c(x)}{T_c(0)} = A - Bx^2 + Cx^4 \,, \qquad \frac{T_c(x)}{T_c(0)} = \frac{a}{\sqrt{1+bx^2}} \,. \tag{8}$$

Results for the local critical temperature (preliminary!)

The coefficients in fits have the following dependence on the linear velocity at the boundary $v_i = \Omega_I R$:

A, B, C, a:

$$c + k v_I^2\,, \tag{9}$$

where

$$k^{(A)} = -0.044 \pm 0.004$$
$$k^{(B)} = 1.275 \pm 0.024$$
$$k^{(C)} = 0.345 \pm 0.025$$

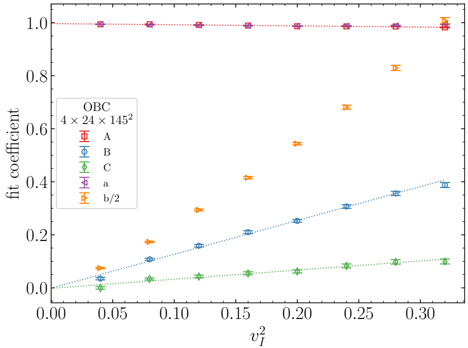

Results for the local critical temperature (preliminary!)

The coefficients in fits have the following dependence on the linear velocity at the boundary $v_i = \Omega_I R$:

A, B, C, a:

$$c + kv_I^2 \,, \tag{9}$$

where

$$k^{(A)} = -0.044 \pm 0.004$$
$$k^{(B)} = 1.275 \pm 0.024$$
$$k^{(C)} = 0.345 \pm 0.025$$

b:

$$c + mv_I^{2p} \,, \tag{10}$$

where

$$m^{(b)} = 4.15 \pm 0.12$$
$$p^{(b)} = 1.263 \pm 0.024$$

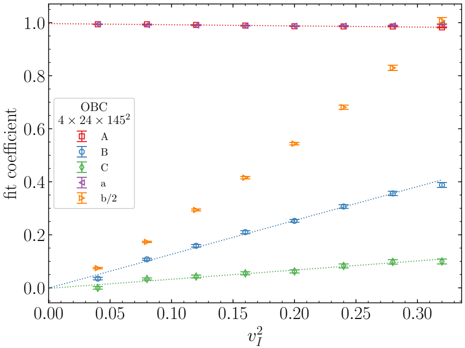

Results for the local critical temperature (preliminary!)

Finally, we obtain

$$\frac{T_c(r,\Omega_I)}{T_c(0)} \simeq 1 - k^{(B)}(\Omega_I r)^2 + k^{(C)}(\Omega_I r)^2 \left(\frac{r}{R}\right)^2 \tag{11}$$

where

$$k^{(B)} = 1.275 \pm 0.024\,, \qquad k^{(C)} = 0.345 \pm 0.025$$

Results for the local critical temperature (preliminary!)

Finally, we obtain

$$\frac{T_c(r,\Omega_I)}{T_c(0)} \simeq 1 - k^{(B)}(\Omega_I r)^2 + k^{(C)}(\Omega_I r)^2 \left(\frac{r}{R}\right)^2 \tag{11}$$

where

$$k^{(B)} = 1.275 \pm 0.024\,, \qquad k^{(C)} = 0.345 \pm 0.025$$

And for another ansatz:

$$\frac{T_c(r,\Omega_I)}{T_c(0)} \simeq \frac{1}{\sqrt{1 + m(\Omega_I r)^2\ (\Omega_I R)^{2p-2}}} \tag{12}$$

where

$$m = 4.15 \pm 0.12\,, \qquad p = 1.263 \pm 0.024$$

(preliminary results from coarse lattice!)

Note, that the Tolman-Ehrenfest effect predict $k^{(B)} = -\frac{1}{2}$ and $k^{(C)} = 0$ or $m = -1$ and $p = 1$.

Mixed-phase diagram

Using the universal results for the local critical temperature, for a given temperature we can find the curve in $(v_I, r/R)$-space, which separate regions with different phases.

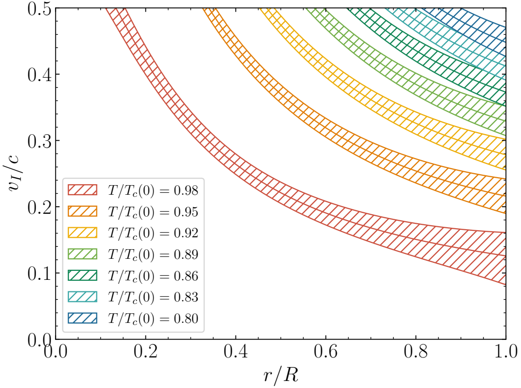

Mixed-phase diagram

Using the universal results for the local critical temperature, for a given temperature we can find the curve in $(v_I, r/R)$-space, which separate regions with different phases.

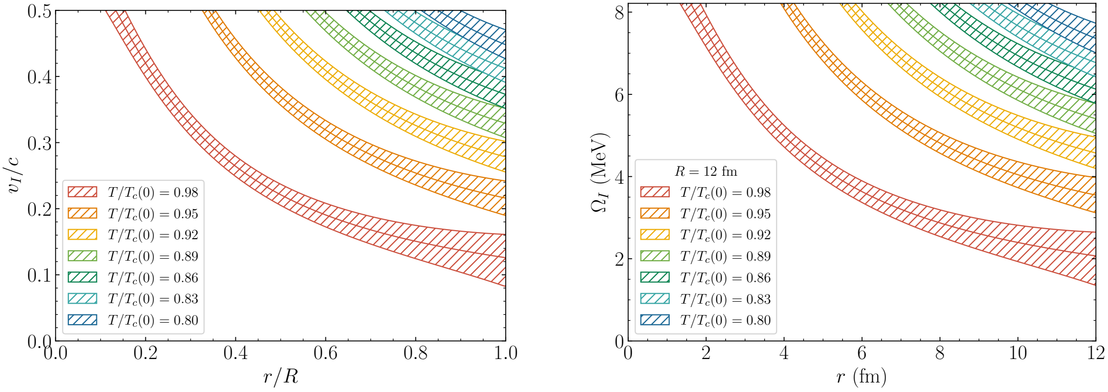

Conclusions

- We found the lattice evidence of the possible state with mixed confinement-deconfinement phases in rotating quenched QCD.
- The local critical temperature is determined mainly by the local linear velocity of rotational motion:

$$\frac{T_c(r,\Omega_I)}{T_c(0)} \simeq 1 - k^{(B)}(\Omega_I r)^2 + \dots \tag{13}$$

where $k^{(B)} = 1.275 \pm 0.024$ (preliminary result for coarse lattice, $N_t = 4$).

- Inhomogeneous phases may appear even for a slow rotation (if the system size is large enough).
- In progress: Simulations with fine lattices, Analytic continuation, etc.

Details coming soon: 2309.XXXXX

Thank you for your attention!

Gluon lattice action

The (improved) lattice gluon action can be written as

$$S_G = \beta \sum_x \Big((c_0 + r^2\Omega_I^2) W_{xy}^{1\times1} + (c_0 + y^2\Omega_I^2) W_{xz}^{1\times1} + (c_0 + x^2\Omega_I^2) W_{yz}^{1\times1} + \\ + c_0 \left(W_{x\tau}^{1\times1} + W_{y\tau}^{1\times1} + W_{z\tau}^{1\times1} \right) + y\Omega_I \left(W_{xy\tau}^{1\times1\times1} + W_{xz\tau}^{1\times1\times1} \right) - \\ - x\Omega_I \left(W_{yx\tau}^{1\times1\times1} + W_{yz\tau}^{1\times1\times1} \right) + xy\Omega_I^2 W_{xzy}^{1\times1\times1} + \sum_{\mu\neq\nu} c_1 W_{\mu\nu}^{1\times2} \Big) , \quad (14)$$

with $\beta = 6/g^2$, and $c_0 = 1 - 8c_1$, where $c_1 = -1/12$ and

$$W_{\mu\nu}^{1\times1}(x) = 1 - \frac{1}{3}\mathrm{Re\ Tr}\ \bar{U}_{\mu\nu}(x) , \quad (15)$$

$$W_{\mu\nu}^{1\times2}(x) = 1 - \frac{1}{3}\mathrm{Re\ Tr}\ R_{\mu\nu}(x) , \quad (16)$$

$$W_{\mu\nu\rho}^{1\times1\times1}(x) = -\frac{1}{3}\mathrm{Re\ Tr}\ \bar{V}_{\mu\nu\rho}(x) , \quad (17)$$

$\bar{U}_{\mu\nu}$ denotes clover-type average of 4 plaquettes,

$R_{\mu\nu}$ is a rectangular loop,

$\bar{V}_{\mu\nu\rho}$ is asymmetric chair-type average of 8 chairs.

Rotating reference frame: temperature

$$\int d^4x \sqrt{g_E}\,(\dots) = \int_0^{1/T} dx_0 \sqrt{g_{44}} \int d^3x \sqrt{\gamma_E}\,(\dots) = \int_0^{1/T} dx_0 \int d^3x \sqrt{g_E}\,(\dots)$$

- Interpretation: Tolman-Ehrenfest effect. In gravitational field the temperature isn't a constant in space at thermal equilibrium:
$$T(r)\sqrt{g_{00}} = const\,,$$
- For the (real) rotation one has
$$T(r)\sqrt{1 - r^2\Omega^2} = const \equiv T\,,$$
- One could expect, that the rotation effectively warm up the periphery of the modeling volume
$$T(r) > T(r=0),$$
and as a result, from kinematics, the critical temperature should decreases.
- Our results show that the behavior of the (pseudo-)critical temperatures is more complicated. It also may be caused by instability.